8.2

Reprinted from Preprint Volume: Eleventh Conference on Severe Local Storms, Kansas City, Missouri, October 2-5, 1979. Published by the American Meteorological Society, Boston, Mass.

OBSERVATIONS OF RELATIONSHIPS BETWEEN TORNADO STRUCTURE, UNDERLYING SURFACE, AND TORNADO APPEARANCE

Gregory S. Forbes

The Pennsylvania State University
University Park, PA 16802

1. INTRODUCTION

This paper presents, in summary form, some observations of tornado structure and behavior. Most of these observations are based upon photogrammetric analyses of the Parker, Indiana tornado of 3 April 1974 and the Cabot, Arkansas tornado of 29 March 1976.

Both the Parker and Cabot tornadoes exhibited remarkable temporal variations in appearance. In the Parker tornado these variations appeared to be primarily a result of changes in tornado structure: the development and evolution of suction vortices. Although the Cabot tornado also contained suction vortices, in several instances the dramatic changes in appearance were directly related to changes in the nature of the underlying surface: grassy field, plowed field, residential area. Accordingly, this paper discusses observations of the complicated interplay between tornado structure, underlying surface, and tornado appearance.

2. CHARACTERISTICS OF THE PARKER TORNADO

The Parker tornado proved to be one of the most interesting tornadoes of the 1974 Superoutbreak because Mr. Wally Hubbard of WISH-TV in Indianapolis obtained a movie of the evolution of this multi-vortex tornado. Based upon the damage path, the tornado was rated F P_L P_W = 4, 3, 4; F4 in intensity and a length of 35 km. The tornado moved toward the north-northeast (about 19 km east of Muncie, Indiana), damaging trees, farms, homes, and a high school. The heaviest damage occurred to buildings immediately north of the school.

The Hubbard movie was used to compute velocities of cloud tags within the suction vortices and the tornado. Details of the technique, and a detailed analysis of the results, are presented by Forbes (1978a). Preliminary results were presented by Forbes (1976), and photogrammetric computations were also performed by Agee et al. (1974).

Figures 1 and 2 illustrate sample computations. In order to measure the flow about the suction vortices, the movie was re-photographed in a suction vortex-fixed frame of reference.

Using techniques outlined by Forbes (1978a), the apparent velocities were separated into components. Table 1 lists the mean and extreme values for each component.

It is interesting to note that the speed of revolution of the suction vortices about the tornado axis was considerably slower than the antecedent tornado tangential velocity. The speed of revolution, however, was considerably faster than that expected due solely to mutual interaction of the suction vortices (about 16 m/s). Furthermore, speeds calculated within the dust clouds associated with the suction vortices suggested that the "steering flow" exceeded the revolution speed by 10 m/s. This suggests that a remnant tornado-scale circulation existed even after suction vortices developed.

If one assumes that the total steering flow acting upon a suction vortex was the sum of flow induced by the other suction vortices and a remnant tornado circulation, calculations indicate that the remnant tornado-scale tangential velocity had a maximum of about 30 m/s. The antecedent tornado circulation, therefore, seemed to exert some control over the speed of suction vortex revolution. (1) There was a remnant tornado circulation (about 60% of the original) present while suction vortices existed. (2) The suction vortices revolved at about 75% of the speed of the total "steering flow".

Figure 3 suggests that the antecedent tornado circulation may exert some control over the tangential velocity of individual suction vortices. Even though computed from totally independent samples, both profiles show similar changes of velocity at corresponding levels.

Table 1

Mean and Extreme Values of Windspeed Components Within the Parker Tornado.

PARAMETER	MEAN (m/s)	MAXIMUM (m/s)
Tornado:		
Tangential	49	82
Radial	≈ 14	58
Vertical	19	44
Translation	24	
Suction Vortex:		
Tangential	39	61
Radial	Not computed	
Vertical	14	36
Revolution	30 on right side	

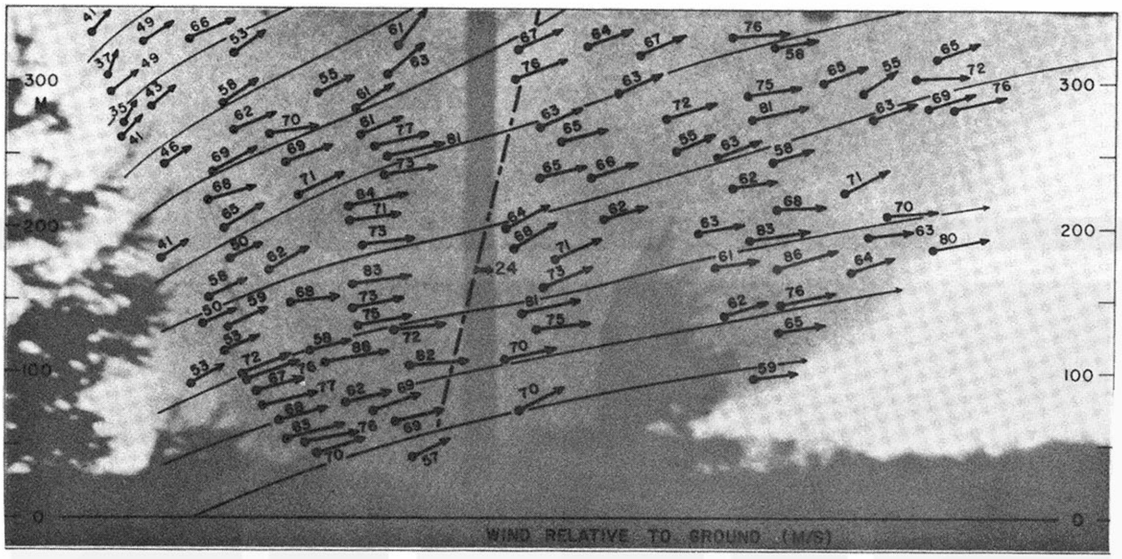

Figure 1. The Parker tornado before suction vortices became visible. Vectors and velocities are of apparent wind with respect to the ground (in m/s), computed from frames 305-317 (0.5 second) of the Hubbard movie.

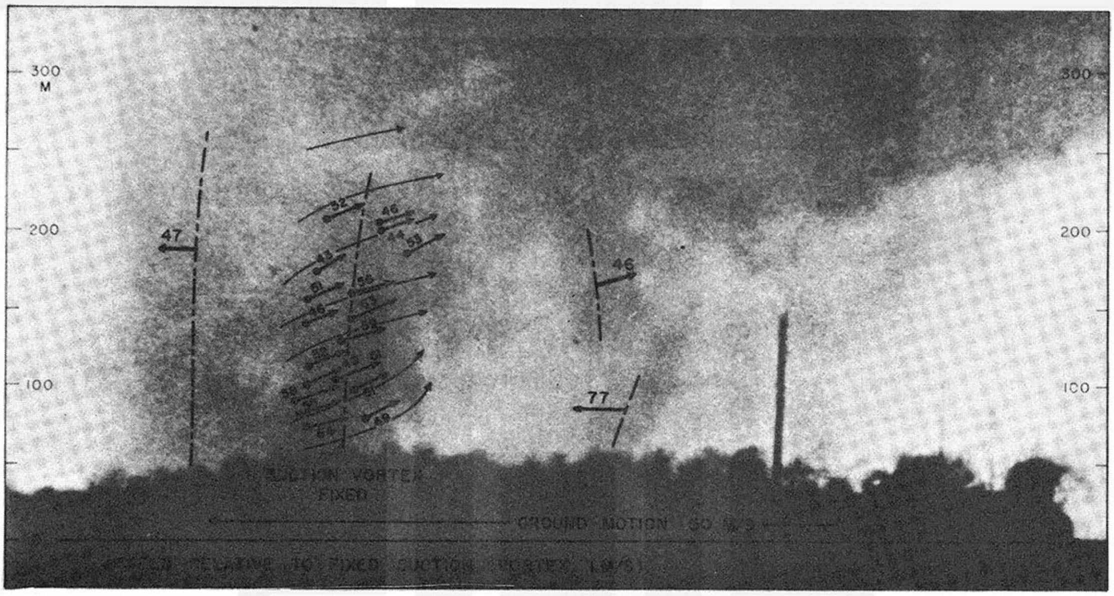

Figure 2. The Parker tornado with suction vortices. The apparent velocities about the vortex are shown (in m/s), as are the speeds of the ground and other vortices relative to this vortex. Computed in a fixed-vortex frame of reference from frames 499-511 (0.5 second) of the Hubbard movie.

3. TORNADO STRUCTURE AND APPEARANCE

Just after Fig. 1, the Parker tornado began to show light (relatively dust-free) areas at low levels within the dust cloud. These light areas were interpreted as signs that the vortex was about to split into multiple vortices. In fact, the tornado appeared to be highly asymmetric even during Fig. 1. Velocities in the left (southeast) side of the tornado are generally faster than those on the right (northeast) side.

Typically there were three or four suction vortices present in the tornado. Suction vortices appeared to form in the left front (northwest) portion of the tornado (orientation relative to its movement), revolve about the rear (south) of the tornado, and lift and dissipate in the right front (northeast) portion of the tornado.

As the tornado approached the high school its appearance began to change from an arrangement of three or four suction vortices to that of a turbulent, chaotic single dust cloud. Subsequently the tornado evolved into an arrangement of two or three suction vortices. The temporary reverse transition toward a turbulent single-vortex tornado may have been related to the increased availability of debris, obscuring the existence of the suction vortices.

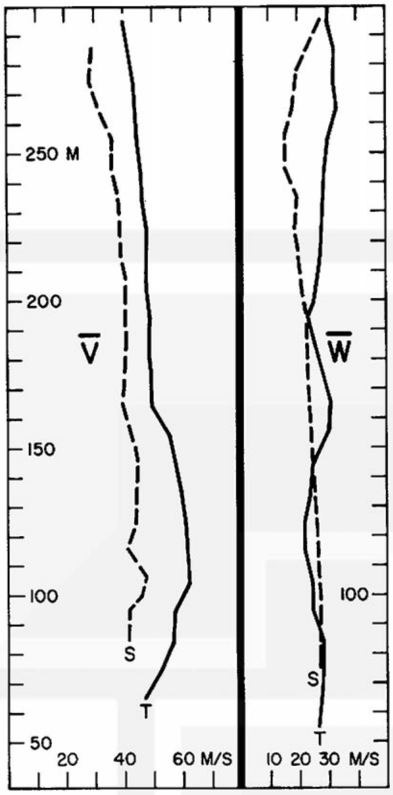

Figure 3. Comparison between the profiles of mean tangential velocity as a function of height for the Parker tornado (T) and the composite suction vortex (S).

Alternatively, the temporary reverse-transition in appearance may have been a manifestation of a change in tornado structure. In laboratory experiments, Leslie (1977) observed that the transition process of increasing the number of multiple vortices was not accomplished merely by developing an additional vortex. Instead, the tornado with N vortices first became turbulent and chaotic (with multiple vortices disappearing) and then re-emerged into a multi-vortex state with N+1 vortices. It is interesting to speculate that this phenomenon occurred in reverse in the Parker tornado, with the chaotic period accompanying the transition from 3 or 4 vortices to 2 or 3 vortices.

Laboratory experiments using a rotating tank (e.g. Weske and Rankin, 1963), in which waves develop in a free-shear layer have shown a relationship between wave number and the lateral extent of the wave. Rough calculations on the basis of nine multiple vortex photos in the literature (Forbes, 1978) indicate that there is a similar relationship for atmospheric vortices:

$$N \cong 1.4 \ (R/a) \ , \qquad (1)$$

where N is the number of suction vortices, R is the radius of maximum winds of the tornado, and a is the radius of the suction vortex. Accordingly, suction vortices are slender (relative to the tornado) when they are numerous.

Laboratory studies have shown that the onset of multiple vortices occurs when a critical value of swirl ratio is reached (Davies-Jones, 1973). This swirl ratio can be related to the ratio of tangential and radial velocity or to the ratio of tangential and mean vertical velocity.

$$S = (V_o/U_o)(r_o/2h) = V_o/\overline{w} \qquad (2)$$

where r_o is the updraft radius and h is the depth of the inflow.

A review of published tornado windspeeds (Forbes, 1978a) reveals that a "poor-man's swirl ratio",

$$S = V_{max}/W_{max} \qquad (3)$$

may be useful in classifying single-vortex and multi-vortex tornadoes. Multi-vortex tornadoes were observed for a range of S of approximately 1.2 to 2.5.

4. CHARACTERISTICS OF THE CABOT TORNADO

The Cabot tornado touched down about 2.4 km north of the western edge of Little Rock Air Force Base (which is located about 20 km northeast of Little Rock, Arkansas). The tornado moved toward the east-northeast and passed through the business district of Cabot, a small community of 3500, at about 1521 CST. After striking Cabot the tornado made a right turn and moved nearly eastward. The total path length was 27 km and the tornado was rated F P_L P_W = 3, 3, 3.

The tornado was photographed extensively during the middle half of its lifetime, including slides of the passage through Cabot. These photos showed the tornado appearance to be quite variable. The condensation funnel extending downward from cloud base rarely reached the ground. In fact, no condensation funnel appeared to exist during the first 11 km of the tornado lifetime, only a slight depression of cloud base. The tornado was detectable primarily because of its dust cloud, which was often broad but exhibited remarkable temporal variations in appearance.

A detailed report on the tornado is given by Forbes (1978b). Figures 4 and 5 give examples of the appearance of the tornado near Cabot.

Donald Beeks took a movie of the tornado when it was located southwest of Cabot. Using this movie, windspeeds were computed photogrammetrically at numerous one-second intervals. Sample results are shown in Figures 6 and 7. The maximum velocities (calculated with respect to the ground) were:

Total Apparent Velocity	64 m/s
Apparent Vertical Velocity	44 m/s
Apparent Horizontal Velocity	60 m/s

Damage during the period of these calculations was rated no higher than F2, which agrees with the calculated windspeeds.

5. UNDERLYING SURFACE AND APPEARANCE

Although the Cabot tornado did undergo many apparent structural changes (i.e. was occasionally multi-vortex), it also changed its appearance as

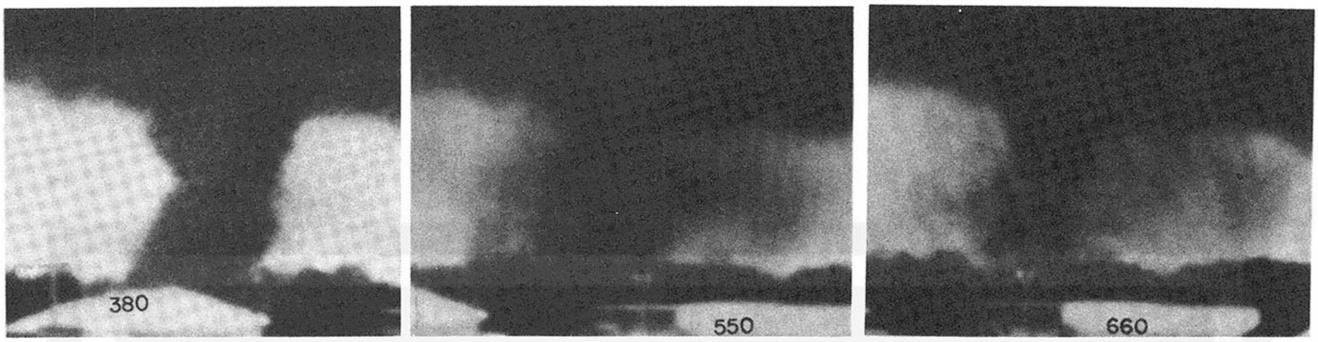

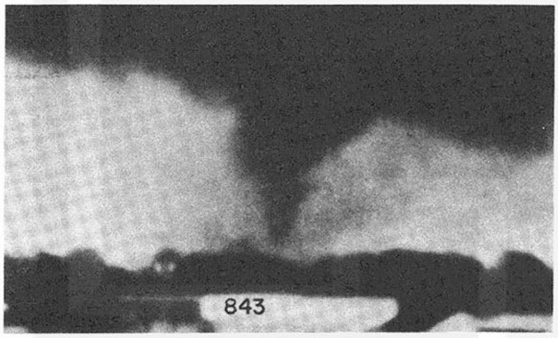

Figure 4. Selected frames from the Beeks movie of the Cabot tornado.

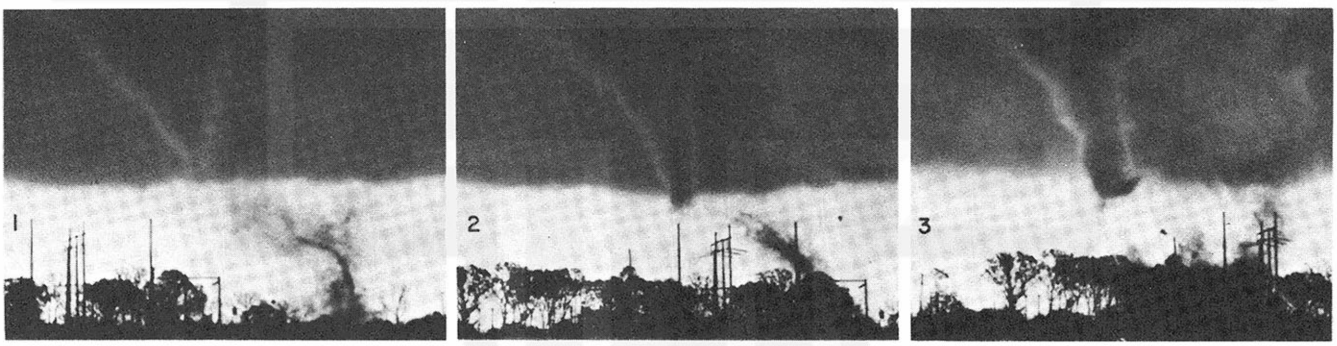

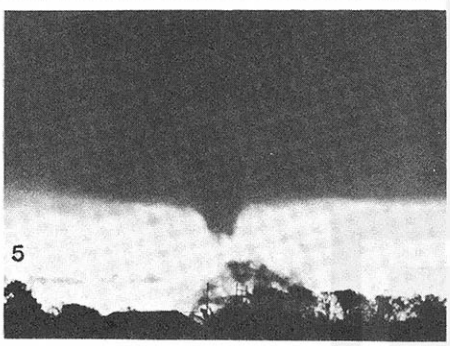

Figure 5. Selected photos of the Cabot tornado, courtesy of Gary Hestir.

it passed over differing types of underlying surface. The shape and extent of the dust/debris cloud was most dramatically affected.

Frame 380 of Fig. 4 shows the tornado as it traversed a forest. After exiting the forest and entering a plowed field (see Fig. 8), the tornado began to develop a large-radius dust cloud.

Frame 550 of Fig. 4 shows that the cylindrical dust cloud/funnel of Frame 380 has largely disappeared and the large-radius dust cloud has emerged. By Frame 660 the tornado had just exited the plowed field and passed into a grass pasture. The dust cloud has already reached its maximum and is beginning to disperse. Most of the dust cloud has diffused by Frame 843.

An examination of Figs. 6 and 7 shows some differences in the observed velocities during this period. In the region about 50 m to the right (ahead) of the tornado axis there are very strong vertical velocities in frame 550, typically about 37 m/s. In that region in frame 660 the velocities were stronger and more horizontal (vertical velocity about 26 m/s).

Although the differing velocity fields of frames 550 and 660 suggest that the tornado structure underwent a change, a more likely explanation is related to the availability of the dust tracers. It appeared that the tracers were not at the same azimuths in frames 550 and 660. Specifically, it appeared that in frame 550 dust was detected rising in the main updraft region. With the dust source removed in frame 660 (note that the region is much lighter), it is likely that the dust tracers are basically rotating around the tornado, and are at a larger radius than in frame 550.

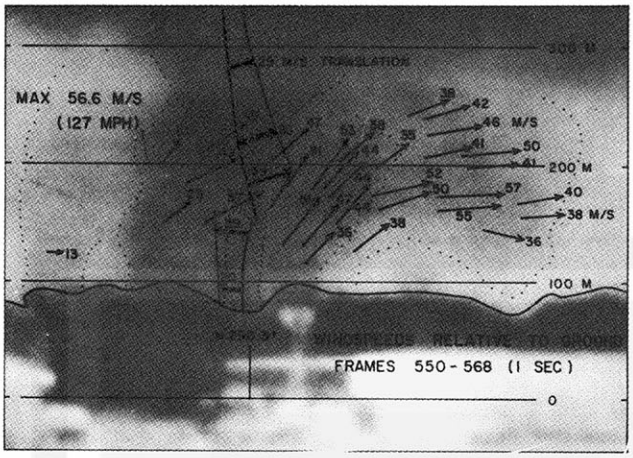

Figure 6. Windspeeds from frames 550-568 of the Beeks movie of the Cabot tornado.

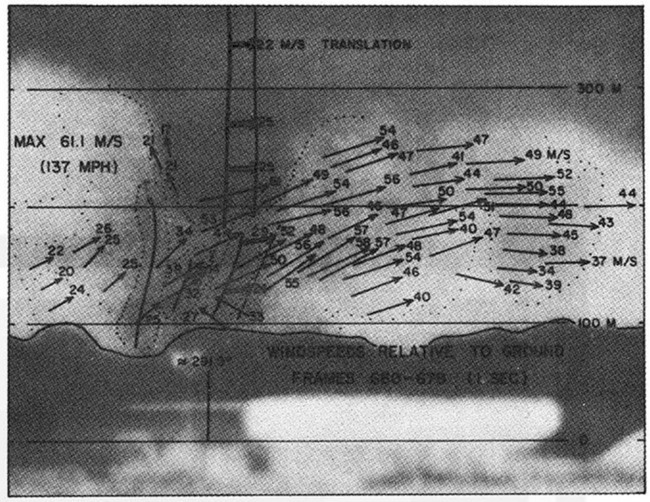

Figure 7. Windspeeds from frames 660-678 of the Beeks movie of the Cabot tornado.

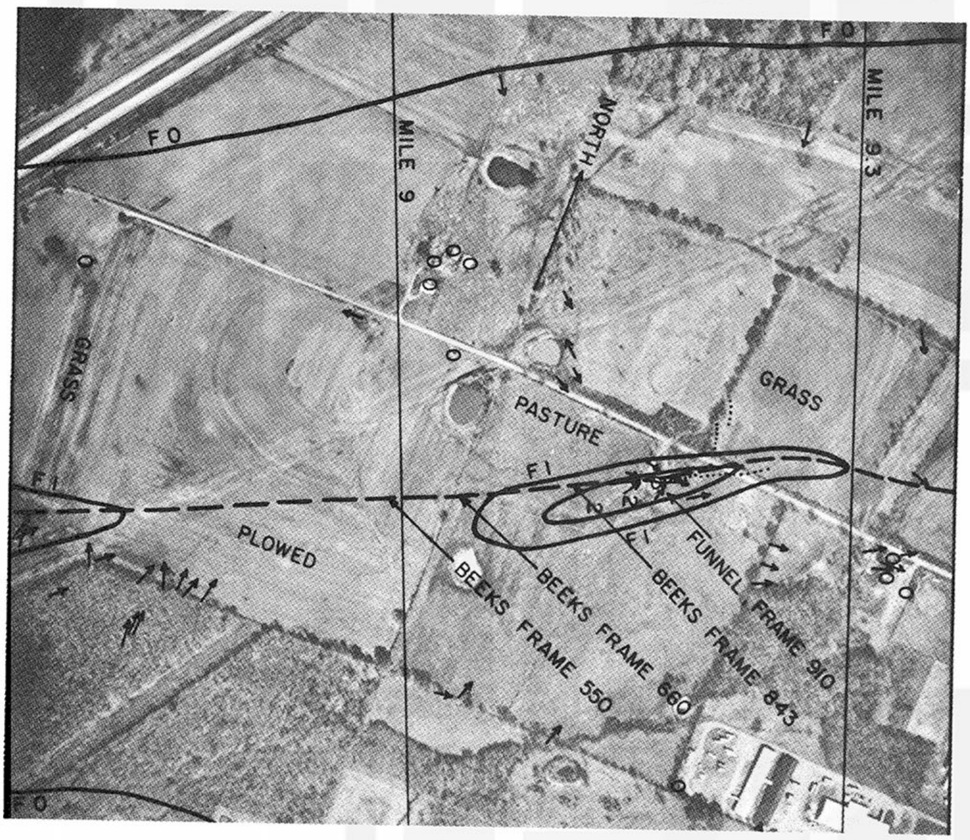

Figure 8. A portion of the Cabot tornado path southwest of Cabot, mapped on an aerial photo taken by the Arkansas Highway Department.

Over residential areas, explosions of buildings can contribute debris to a dust/debris cloud. As the debris rises, the tornado may appear to have layers of debris, as in photo 5 of Fig. 5.

The underlying surface did not exert any obvious control over the existence of suction vortices, which occurred sporadically throughout much of the tornado lifetime.

When the photos of the tornado were related to the damage path, suction vortices did not appear to correspond well to loops of debris present on the grass airfield west of Cabot.

Suction vortices corresponded fairly well to swaths of building damage, however. Refer to photos 1-3 of Fig. 5 and the aerial damage photo of Fig. 9. Photos 1 and 2 both show basically a single suction vortex, with possibly a second suction vortex in very close proximity. Alternatively, photo 2 may be showing the core structure of a single suction vortex -- dense walls and a transparent interior. Photo 3 appears to show three suction vortices, but the correlation between individual suction vortices and damage swaths is not clear-cut. It is interesting to note the pronounced lag of the suction vortices behind the funnel aloft.

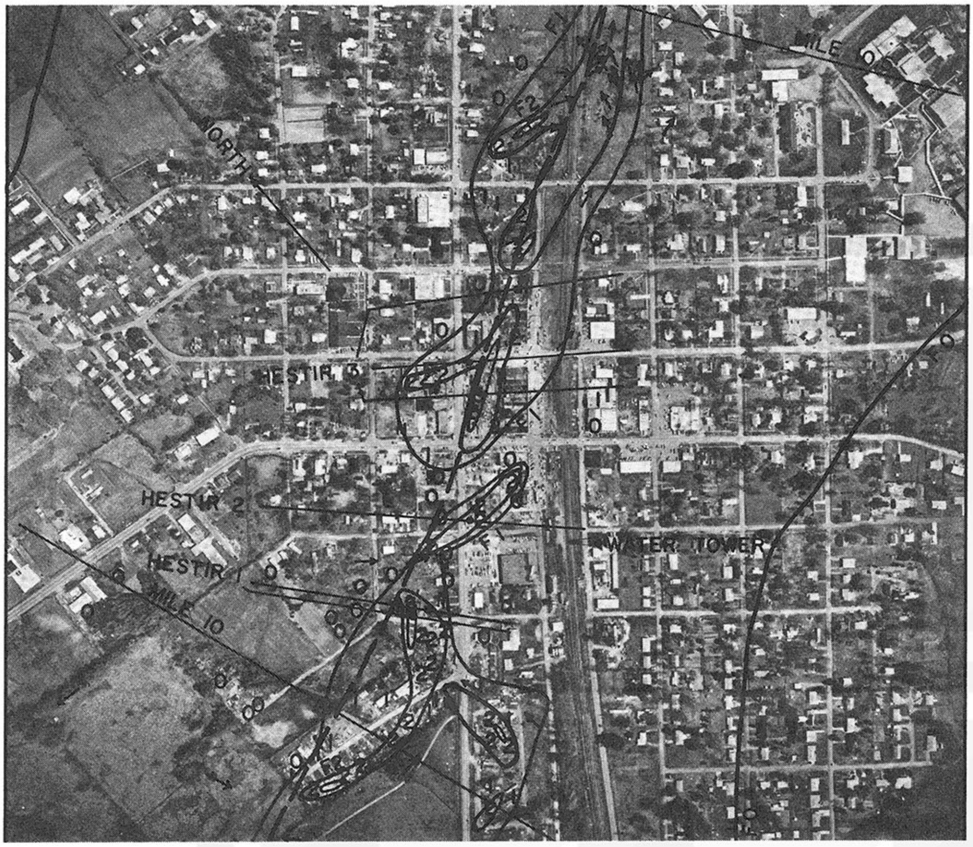

Figure 9. Path of the tornado across downtown Cabot, mapped on an Arkansas Highway Department photo.

6. DOWNBURSTS AND TORNADO STRUCTURE

Fujita (1978) has shown that downbursts often occur in the proximity of tornadoes. In fact, downbursts may instigate tornado formation, changes in tornado movement, and even tornado dissipation (presumably when the downburst is exceedingly strong and cold). Downbursts were detected on the right side of both the Parker and Cabot tornadoes, although they did not appear to be strong.

Downbursts occurred during the latter quarter of the lifetime of the Cabot tornado. During this time the tornado was poorly organized, with the core of strong damage sporadically disappearing and re-appearing. The downbursts, with winds from the south, occurred in regions where the strong tornado damage disappeared. The tornado appeared to oscillate along its course during this time, with the path exhibiting slight sinusoidal tendencies.

ACKNOWLEDGEMENTS

Most of the research was performed at the University of Chicago. The author appreciates the suggestions of Prof. T. T. Fujita of the University of Chicago and Robert F. Abbey, Jr., of the U. S. Nuclear Regulatory Commission. This research was performed under NRC Contract 04-74-239.

The author is grateful to: Wally Hubbard, who provided the Parker movie; Donald Beeks, who provided the Cabot movie; Gary Hestir, who provided the Cabot photos; Arkansas Highway Department, which provided aerial damage photos.

REFERENCES

Agee, E. M., C. Church, C. Morris, and J. T. Snow, 1975: Some synoptic aspects and dynamic features of vortices associated with the tornado outbreak of 3 April 1974. Mon. Wea. Rev., 103, 318-333.

Davies-Jones, R. P., 1973: The dependence of core radius on swirl ratio in a tornado simulator. J. Atmos. Sci., 30, 1427-1430.

Forbes, G. S., 1976: Photogrammetric characteristics of the Parker tornado of April 3, 1974. Proc. Symposium on Tornadoes. Texas Tech. Univ., Lubbock, pp. 58-77.

Forbes, G. S., 1978a: Three scales of motions associated with tornadoes. U. S. Nuclear Reg. Comm., NUREG/CR-0363.

Forbes, G. S., 1978b: The Cabot, Arkansas tornado of March 29, 1976. The Univ. of Chicago SMRP Res. Paper No. 167.

Fujita, T. T., 1978: Manual of downburst identification for Project NIMROD. SMRP Res. Paper No. 156, The Univ. of Chicago, 104 pp.

Leslie, F. W., 1977: Surface roughness effects on suction vortex formation: a laboratory simulation. J. Atmos. Sci., 34, 1022-1027.

Weske, J. R. and T. M. Rankin, 1963: Generation of secondary motions in the field of a vortex. Phys. Fluids, 6, 1397-1403.